Pacific Northwest
NATIONAL LABORATORY

PNNL-36741

# Enabling Ultralow Volume Analysis with a High-Resolution Ion Mobility Mass Spectrometry Platform

September 2024

Adam L. Hollerbach
Yehia M. Ibrahim
Randolph V. Norheim
Gordon A. Anderson
Adam G. Ryan
John Lindquist

U.S. DEPARTMENT OF ENERGY

Prepared for the U.S. Department of Energy
under Contract DE-AC05-76RL01830

## DISCLAIMER



PACIFIC NORTHWEST NATIONAL LABORATORY
*operated by*
BATTELLE
*for the*
UNITED STATES DEPARTMENT OF ENERGY
*under Contract DE-AC05-76RL01830*

**Printed in the United States of America**

**Available to DOE and DOE contractors from**
**the Office of Scientific and Technical Information,**
**P.O. Box 62, Oak Ridge, TN 37831-0062**
**www.osti.gov**
**ph: (865) 576-8401**
**fox: (865) 576-5728**
**email: reports@osti.gov**

**Available to the public from the National Technical Information Service**
**5301 Shawnee Rd., Alexandria, VA 22312**
**ph: (800) 553-NTIS (6847)**
**or (703) 605-6000**
**email: info@ntis.gov**
**Online ordering: http://www.ntis.gov**

PNNL-36741

# Enabling Ultralow Volume Analysis with a High-Resolution Ion Mobility Mass Spectrometry Platform

September 2024

Adam L. Hollerbach
Yehia M. Ibrahim
Randolph V. Norheim
Gordon A. Anderson
Adam G. Ryan
John Lindquist

Prepared for
the U.S. Department of Energy
under Contract DE-AC05-76RL01830

Pacific Northwest National Laboratory
Richland, Washington 99354

# Abstract

Of all the molecules thought to exist in the universe, it is estimated that researchers only know the chemical structures of 5% of them. Identifying the chemical structures of the remaining 95% has proven extremely challenging because many molecules exhibit low abundance, are contained in small volumes (e.g., <10 nL), do not readily ionize, exhibit similar structures to other molecules, etc. No single analytical technique exists to definitively identify the structure of an unknown molecule, and thus multiple different molecular measurements are typically made (i.e., multi-modal approach). Ion mobility (IMS) and mass spectrometry (MS) are two key tools that researchers use to determine the chemical structures of unknown molecules, and recently high-resolution and ultrahigh resolution IMS-MS instruments have provided greater confidence than ever before. However, HR-IMS-MS instruments typically exhibit low ion utilization efficiency, meaning they require large amounts of sample for an analysis (e.g., >10 µL). Unfortunately, this limitation prohibits the analysis of small volume samples where many unknown molecules exist. Described herein are the efforts made to enable the analysis of ultralow volumes with an HR-IMS-MS platform. A new scanning technique, termed a 'stuttered traveling wave scan', was developed as a replacement for the dual-gated scanning technique and works by halting the traveling waves after allowing ions to separate and then repeatedly restarting and stopping the traveling waves to incrementally move ions from the SLIM to the Orbitrap. Ions were stored inside the SLIM while the TWs were stopped, allowing the Orbitrap to perform high-resolution mass analysis. When the Orbitrap was ready, the TWs were restarted for short periods of time (<10 ms) to move ions from the SLIM to the Orbitrap. It was discovered that lower TW amplitudes and speeds than used during IMS separation were required to produce IMS peaks with the highest signal intensities and best resolving powers. The stuttered TW scan was found to produce similar resolutions and signal intensities compared to the dual-gated scanning technique. A new IMS design possessing an intersecting 'tee' with a reversible traveling wave was also developed to improve ion utilization efficiency during cyclic operation, which is necessary when only a single IMS spectrum can be acquired, such as when analyzing ultralow volume samples. The new capabilities described in this report lay the groundwork for acquiring HR-IMS-MS spectra of ultralow volume biological samples, such as single cells, where HR-IMS-MS can help elucidate the structures of unknown compounds.

# Summary

This report describes a new high ion utilization efficiency ion mobility separation method that allows ultralow volumes of sample to be analyzed with a high-resolution ion mobility / high-resolution mass spectrometry platform. A new ion mobility design provided enhanced ion utilization efficiency during cyclic IMS experiments, and a new traveling wave-based scanning method established a way to analyze all the ions injected into the ion mobility spectrometer. The ability to analyze all the ions from a single injection provides a foundation for analyzing ultralow volume samples, such as single cells.

# Acknowledgments

This research was supported by the Strategic Investments Program, under the Laboratory Directed Research and Development (LDRD) Program at Pacific Northwest National Laboratory (PNNL). PNNL is a multi-program national laboratory operated for the U.S. Department of Energy (DOE) by Battelle Memorial Institute under Contract No. DE-AC05-76RL01830.

# Contents



# Figures

# 1.0 Introduction

Ion mobility-mass spectrometry (IMS-MS) hybrid instruments are well suited for helping researchers identify the chemical structures of unknown molecules in mixtures because they provide three complimentary types of measurements: chemical formula, fragmentation pattern, and collision cross section (CCS).( Blaženović et al. 2018, 10758-64; Luo et al. 2023) However, a concern when developing IMS-MS instruments is how to efficiently couple the IMS to the MS without sacrificing the performance of either. Many IMS measurements take 200 ms or less to complete, which means that even faster MS analysis is required to ensure that all the features contained within the IMS separation are captured. The most common MS systems to use alongside IMS are time-of-flight (TOF-MS) because they require less than 200 µs to perform a mass scan, which is ~1000x faster than most IMS separations. IMS is less frequently coupled to other MS systems like quadrupoles, ion traps, Orbitraps, and Fourier transform ion cyclotron resonance (FTICR) because they require 1 ms or more to perform a single mass measurement. These slower MS scan rates can under sample spectral features from the IMS and cause useful information to be lost. For example, a single high-resolution Orbitrap scan at 140k mass resolution can take one second to complete, but since many IMS separations are completed in less than 200 ms, the IMS separated ions will simply accumulate in the Orbitrap and be mass analyze all at once. Most IMS separations cannot be slowed down to give the MS more time to complete a mass analysis, although examples of slowed down IMS separations using trapped ion mobility spectrometry (TIMS) coupled to an FTICR-MS have been reported by Pu et al.(Pu et al. 2016, 3440-3). It is therefore important to consider how an IMS and high-resolution MS can be coupled without sacrificing the resolution of either instrument.

One way to couple IMS to slow MS instruments is to use the dual-gated scanning technique.(Karasek, Hill, and Kim 1976, 327-36; Hollerbach, Fedick, and Cooks 2018, 13265-72) The dual-gated scanning technique is straightforward to implement and only requires that one additional ion gate be placed inside a conventional IMS after the separation stage. To perform the dual-gated scanning technique, the first ion gate is used to perform conventional ion injections while the second ion gate is scanned in small increments after a time delay to transmit portions of completed IMS separations to the MS. The mass spectra obtained by scanning the second ion gate are stitched together in postprocessing to generate an IMS spectrum that maintains the resolution of both the IMS and the MS. The main attraction of the dual-gated scanning technique is that it allows most IMS and MS to be coupled together while maintaining the resolution of both systems. This is especially important when coupling two high resolution IMS and MS systems, such as a recently developed structures for lossless ion manipulations (SLIM) Orbitrap MS platform.(Hollerbach et al. 2023, 9531-8) The SLIM-Orbitrap has tremendous potential for identifying unknown ions that cannot currently be achieved with other IMS-MS systems, and dual-gated scanning technique has enabled such HR-IMS-MS/MS experiments to be performed.

Unfortunately, the traditional dual-gated scanning technique has two well-known limitations: (1) long analysis times, and (2) low ion utilization efficiency (e.g., 0.01% duty cycle). These limitations prevent dual-gated scanning instruments, such as the SLIM-Orbitrap, from being used to analyze low volume samples (e.g., <1 µL) or from being coupled to pulsed ion introduction sources like atmospheric pressure chemical ionization (APCI), thermal desorption, and dielectric barrier discharge ionization (DBDI). This is unfortunate because HR-IMS and HR-MS instruments are essential in many analytical workflows for helping determine the identifies of unknown compounds. However, the dual-gated scanning technique is not the only way to couple a SLIM to an Orbitrap. Implementing a new coupling method, such as one that utilizes traveling waves, would allow HR-IMS-MS to be performed with near 100% high ion utilization efficiency (near

100%) and overcome the need to use large amounts of sample, which is necessary when working with ultralow volume samples and pulsed ionization sources. Such a powerful capability will allow for much deeper dives into biological analysis and will greatly expand on the types of samples that can be analyzed with HR-IMS-MS/MS.

This report describes the development of a new high ion utilization efficiency IMS separation method that enables high-resolution IMS, high-resolution MS, and MS/MS spectra of ultralow volumes of sample to be acquired simultaneously. The method is termed a “stuttered TW scanning method” and works by iteratively stopping and restarting the TWs inside a SLIM to sample portions of completed IMS separations. The stuttered TW scanning method can be used as a replacement to the dual-gated scanning technique for coupling fast TWIMS separations to slow MS analyzers. The method was demonstrated inside a new high ion utilization efficiency SLIM design using mixtures of stable standard compounds. The challenges associated with the stuttered TW scanning method are outlined and suggestions for future work are made to fully harness the potential of the high ion utilization efficiency SLIM system for ultralow volume sample analysis, such as for analyzing single cells.

# 2.0 Experimental Details

## 2.1 Chemicals and Electrospray Ionization

All peptides (SDGRG, GRGDS, kemptide, angiotensin I, bradykinin, neurotensin, angiotensin II, renin substrate tetradecapeptide porcine, melittin, substance P, fibrinopeptide A) and HPLC grade acetonitrile were purchased from Millipore-Sigma (St. Louis, MO, USA). Melittin was received at > 85% purity, GRGDS and neurotensin at > 90% purity, and all other peptides at > 93% purity. The reverse peptide and standard peptide solutions were prepared to 2 µM and 1 µM equimolar solutions, respectively, in 1:1 water:acetonitrile with 1% acetic acid (49.5% / 49.5% / 1%). Ionization was performed using nanoelectrospray emitters that were pulled from borosilicate glass capillaries with a Sutter flaming / brown micropipette tip puller (model P-1000, Sutter Instrument, Novato, CA, USA). The outer diameters of all emitters ranged from ~2-6 µm and were measured using a camera with a 10x microscope objective. The nanoelectrospray emitters were mounted on a holder with a steel wire threaded through the middle. A high DC voltage (~2 kV) was applied to the steel wire to ionize all solutions.

## 2.2 Instrumentation and Electronics

All IMS-MS experiments were performed using a previously described SLIM-Orbitrap system, which is comprised of an 11-meter SLIM module coupled to a Q-Exactive Orbitrap MS.(Hollerbach et al. 2023, 9531-8) Nitrogen was the buffer gas. All TWs were sine waves. The SLIM board layout used in this study was modified from previous studies in that the ion switch (Garimella et al. 2015, 6845-52) located at the end of the SLIM was replaced with a tee region (**Figure 1**). A separate TW was applied to the tee region and its direction was used to send ions to the Orbitrap (forward motion) or to the reroute path (reverse motion) without requiring a DC blocking voltage. The effects of TW phasing on ion transmission in this tee region is discussed later. Dual-gated IMS-MS experiments were performed as previously described.(Hollerbach et al. 2023, 9531-8) All traveling waves and DC voltages were generated using a modular intelligent power supply (MIPS, GAA Custom Engineering LLC, Kennewick, WA, USA). In-house built power supplies provided high voltage radiofrequencies (RF) to the first two ion funnels in the system and the SLIM. The MIPS also supplied RF to the rear ion funnel.

## 2.3 Stuttered traveling wave scan

A new scanning technique termed a ‘stuttered traveling wave scan’ was developed as an alternative way to couple an IMS to a slow MS and to provide a way to analyze ultralow volume samples with an IMS-HR-MS. To help describe how the new stuttered traveling wave scanning method works, a timing diagram is provided in **Figure 2**. The ejection signal from the C-trap of the Orbitrap was used to trigger all IMS separations (**Figure 2**, top) and was set to 1 Hz (AGC set to 'fixed' status). To start an IMS experiment, a single pulse from the C-trap caused ions to be injected from the second ion funnel into the SLIM (**Figure 2**, bottom). Note that the timing diagram represents the voltages applied to a single TW electrode (e.g., one TW electrode out of a set of eight). The other seven TW electrodes will exhibit identical voltage profiles except that they will be phase shifted. During ion injection, the amplitudes of all traveling waves were lowered to facilitate ion transfer to the SLIM. Square waves are used in this illustration, but any waveform shape can be used (e.g., sine, triangle, sawtooth, custom). After the ion injection step, the amplitudes of the TWs were increased to begin IMS separations. The process of using low TW amplitudes during ion injections and high TW amplitudes during IMS separations is known as ‘in-SLIM accumulation’ and has been described previously.(Wojcik et al. 2019, 11953; Hollerbach et

al. 2023, 9533) Ions were allowed to separate inside the SLIM for a specified time (e.g., 200 ms) using conventional TW conditions. After this specified time, the TWs were then stopped, which caused ions to stop moving inside the SLIM and become trapped in place. This is the beginning of the 'stuttered' portion of the new scanning method. While the TWs were stopped, ions were prevented from diffusing radially inside the SLIM by the RF and guard electrodes, and the stopped TWs prevented ions from diffusing lengthwise along the SLIM tracks. Any ions that exited the SLIM before the TWs were stopped were mass analyzed by the Orbitrap. After receiving another trigger signal from the C-trap, the TWs were momentarily restarted, which allowed ions to resume traveling through the SLIM for a short time (e.g., 10 ms). The length of time that the TWs were restarted for is termed the 'stutter on-time', and this term will be used for the remainder of the study. Any ions that exited the SLIM during this short time were sent to the Orbitrap for mass analysis. Note that the restarted TWs in **Figure 2 bottom** are displayed as having a slower speed and lower amplitude than the separation TW. The reasons for using slower TW speeds and lower TW amplitudes is discussed later, but in summary, optimal peak shapes and IMS resolutions are obtained when these TW parameters are used during the stutter on-time step. After the short stutter on-time, the TWs were stopped again, which again caused any ions inside the SLIM to become trapped while ions that exited the SLIM were mass analyzed by the Orbitrap. The process of restarting and stopping the TWs can be repeated any number of times (denoted by 'n') until all desired ions have been sent to the Orbitrap. After the stuttering process is complete, the TWs were restarted for 1000 ms to empty the SLIM of any remaining ions. One benefit of this new stuttering TW scanning method is that it allows small portions of the SLIM separations to be analyzed with the Orbitrap while it performs high resolution mass analysis. The stuttered TW scanning method therefore provides an alternative approach to the dual-gated scanning technique for coupling a TW-based IMS to a slow scanning MS.(Hollerbach et al. 2023, 9531-8)

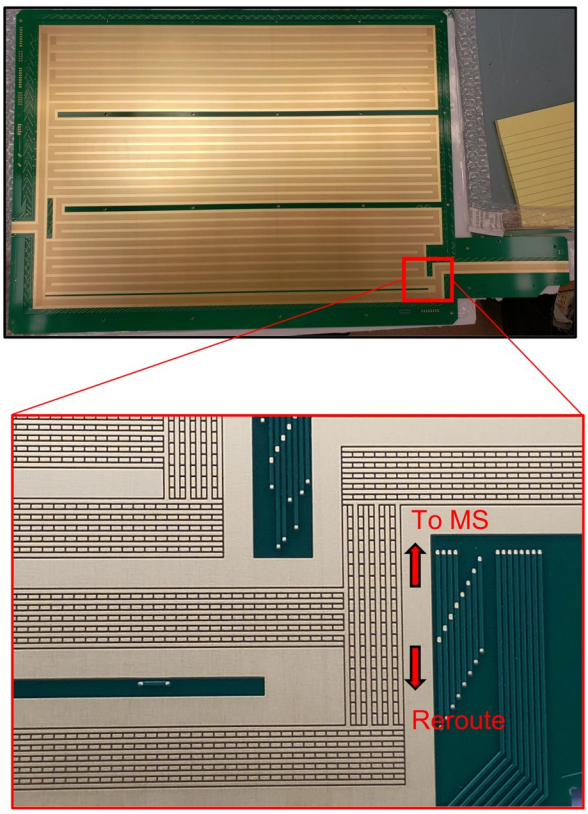


Figure 1: Photographs of the top the bottom SLIM board containing a tee region in place of an ion switch. A TW with a reversible direction was applied to the tee to move ions to the MS or to the reroute path for extra IMS separation.

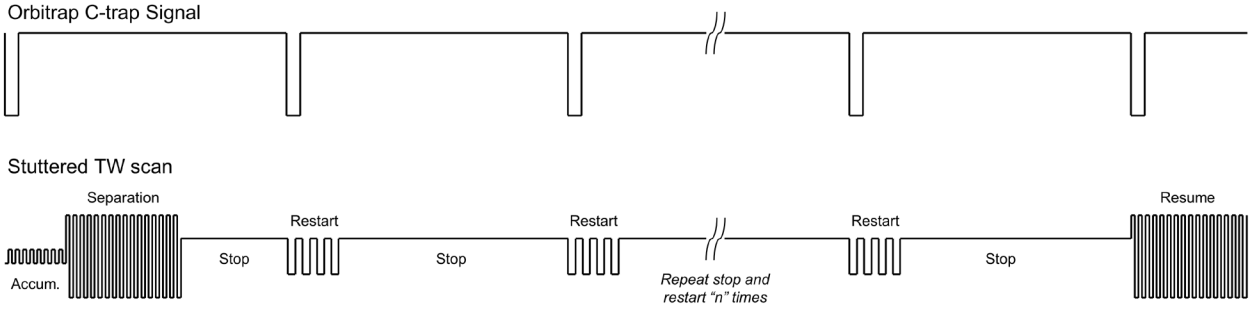


Figure 2: Timing diagram of the stuttered TW scanning method.

# 3.0 Results and Discussion

## 3.1 Evaluation of a stuttered TW scanning method

The new stuttered TW scanning method was first evaluated by acquiring IMS-MS spectra of a mixture of two reverse peptides ($SDGRG^{1+}$, $GRGDS^{1+}$). The power supply was programmed to perform back-to-back IMS separations with the stuttered TW scanning method, and a plot of the total ion mobilogram of five IMS separations is shown in **Figure 3A**. The plot showed six high intensity peaks and ten lower intensity peaks located between the high intensity peaks. The high intensity peaks corresponded to ions arriving before the TWs were first stopped and ions arriving after the stuttering process was complete. The lower intensity peaks corresponded to the two reverse peptides. To acquire these IMS separations, ions were allowed to separate for 295 ms before the TWs were halted. The stuttering process was then performed thirty-five times, and the SLIM was emptied on the thirty-sixth scan. Since each scan took one second, the total time to sample an IMS separation with a stuttered TW scan operating under the previously mentioned conditions was thirty-six seconds. Note that the x-axis was plotted as scan number because an ion's relationship to arrival time was not completely known.

An average of the five IMS separations was taken and a plot of the extracted ion mobilogram (EIM) of *m/z* 491 was generated to better view the reverse peptide peaks (**Figure 3B, blue trace**). Baseline-separation was obtained for the two reverse peptides. The peak-peak resolution of the reverse peptides was calculated according to equation 1:

$$\text{Resolution}_{\text{pp}} = \frac{1.18 * (\text{td}_2 - \text{td}_1)}{\text{fwhm}_2 + \text{fwhm}_1} \quad (1)$$

where $td_2$ and $td_1$ are the peak centers and $fwhm_1$ and $fwhm_2$ are the full-width at half maxima of the peaks. The resolution was calculated to be 2.18. For comparison, an average of five dual-gated SLIM-Orbitrap separations was acquired using the same mixture (**Figure 3B**, red trace) and the resolution of the two reverse peptides was calculated to be 2.02. The resolutions are similar and indicates that the new stuttered TW scanning method can perform similarly to the dual-gated scanning method while allowing high-resolution mass analysis to be performed (**Figure 3C**). The difference in resolutions is attributed to the fact that the dual-gated scanning method produced peaks with slightly higher signal intensities and wider peaks than the peaks obtained with the stuttered TW scanning method.

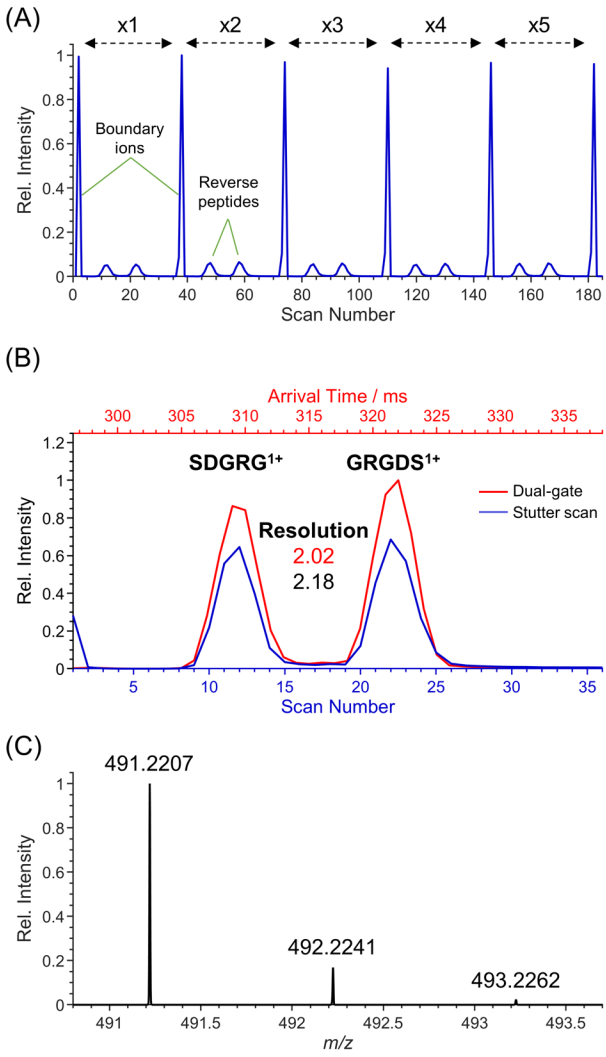


Figure 3: (A) Total ion mobilogram showing five IMS separations of two reverse peptides collected using the stuttered TW scanning method. (B) Extracted ion mobilogram of *m/z* 491 collected over an average of five IMS separations using the stuttered TW scanning method (black trace) and a dual-gated scanning method (red trace). (C) HR-MS$^1$ of the isotopic envelop of the reverse peptides. $TW_{accum}$ = 104 m/s, 1 $V_{0\text{-}p}$, 200 ms. $TW_{sep}$ = 104 m/s, 17.5 $V_{0\text{-}p}$. $TW_{stutter}$ = 32 m/s, 5 $V_{0\text{-}p}$, 10 ms / 1 s. Guard = +15 $V_{dc}$. SLIM pressure = 2.26 Torr nitrogen.

## 3.2 Optimization of the stuttered TW scanning method

Experiments were performed to determine how the quality of the IMS separation was affected by the length of time ions were allowed to separate before the TWs were stopped for the first time (see Figure 2, bottom labeled *separation*). **Figure 4A** shows five overlaid EIMs of *m/z* 491 acquired using initial SLIM separation times of 100 ms (red trace), 150 ms (green trace), 200 ms (blue trace), 250 ms (orange trace), and 300 ms (purple trace). Note that a normalized x-axis was used because ions took longer to exit the SLIM when short initial separation times were used versus when long initial separation times were used. Peaks with the highest intensities and narrowest widths were obtained when separation times were longer. The highest quality IMS separations were obtained when 300 ms of initial separation time was used. This data suggests that ions that are stopped far away from the exit of the SLIM will exhibit lower resolutions than

ions stopped near the exit of the SLIM. This can be explained by considering that low mobility ions will not have undergone as much IMS separation as high mobility ions.

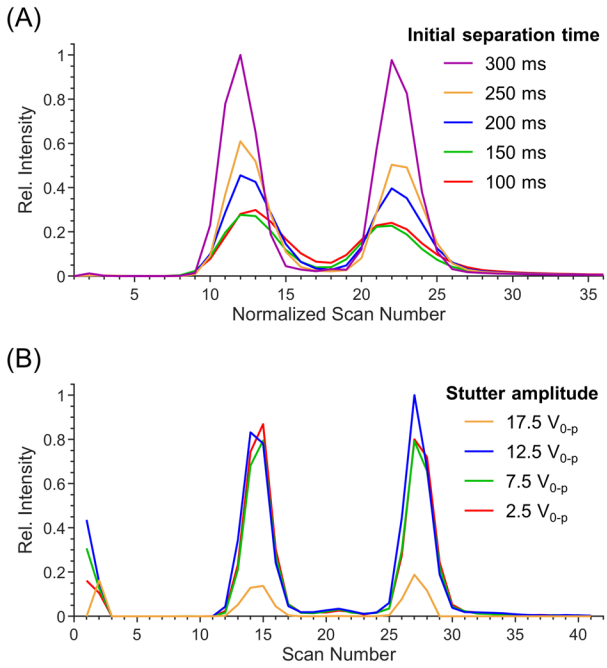


Figure 4: (A) Overlaid EIMs of *m/z* 491 acquired as a function of the initial separation time. $TW_{accum}$ = 104 m/s, 1 $V_{0\text{-}p}$, 100 ms. $TW_{sep}$ = 104 m/s, 17.5 $V_{0\text{-}p}$. $TW_{stutter}$ = 64 m/s, 5 $V_{0\text{-}p}$, 10 ms on-time. Pressure = 2.27 Torr nitrogen. 5 scans per average. (B) Overlaid EIMs of *m/z* 491 acquired as a function of stuttered TW amplitude. $TW_{accum}$ = 104 m/s, 1 $V_{0\text{-}p}$. $TW_{sep}$ = 104 m/s, 17.5 $V_{0\text{-}p}$. $TW_{stutter}$ = 8 m/s, 6 ms on-time.

A systematic study was also performed to determine the effect that TW speed, amplitude, and on-time had on the quality of IMS separation. The effects of using four different stutter TW amplitudes while holding the TW speed and on-time constant (8 m/s, 6 ms) are shown in **Figure 4B**. The results showed that higher stutter TW amplitudes produced low intensity peaks (e.g., 17.5 $V_{0\text{-}p}$, orange trace) while lower amplitudes produced higher intensity peaks. Note that these data were collected using a low stutter TW speed, and other studies showed that using different stutter TW speeds required different TW amplitudes to produce the highest intensity peaks. This interplay observed because the effects of stutter TW speed, amplitude, and on-time cannot be completely decoupled from each other. TW speed and amplitude contribute to whether ions are moving under separation or surfing conditions, and ions will require different on-times depending on the speed of the TW. In general, it was found that using lower TW speeds and amplitudes during the on-time of the stuttered TW scan produced IMS peaks with higher signal intensities and more Gaussian-shaped profiles than if higher TW speeds and amplitudes were used, such as the TW parameters used for separation. In fact, no IMS peaks were observed when the stutter TW and separation TW parameters were kept the same, even when short on-times were used (e.g., 1 ms).

Some logic can be applied to explain why the stutter TW required different conditions than the separation TW to produce optimal IMS signal intensities and peak shapes. There should be an interplay between how fast the TWs are moving and how long the stutter TW can be enabled before it is stopped. If a fast TW (at sufficiently high amplitude) is used for a long time, all ions

comprising a peak should be sent to the Orbitrap during a single stutter on-time event, meaning that the peak would be collapsed into a single data point. It also seems likely that ions would undergo additional rollover events if the stutter TW was sufficiently fast and/or possessed low amplitudes. Ions that would have comprised a peak would instead undergo additional IMS separation and/or diffusion, which would result in the loss of peak shape and signal intensity. Therefore, the optimal TW conditions to use during the stutter TW scanning method are slow TW speeds and low TW amplitudes.

## 3.3 Faster total experiment times when IMS separations are longer than Orbitrap injection times

One of the reasons the stuttered TW scanning method was developed was to create a new way to couple fast IMS separations with slow MS analysis speeds while achieving high ion utilization efficiency. The stuttered TW scanning method also has the potential to provide faster total experiment times if the IMS separation time is longer than the MS analysis time, but it is not so long that the MS can be used to adequately sample across all IMS peaks. When using SLIM, long IMS separation times often occur when ion cycling (or multilevel) experiments are performed, which are designed to provide additional IMS path length to resolve ions with similar CCSs. A disadvantage of using the dual-gated scanning technique with the SLIM-Orbitrap is that the Orbitrap's injection time must be set equal to the total SLIM separation time because the injection signal is used to trigger subsequent IMS injections. The injection time can reach many seconds depending on the length of the SLIM separation. However, the stutter TW scanning method does not require the injection time of the Orbitrap to be simultaneously increased with SLIM separation time because the stutter TW scanning method does not require an entirely new IMS separation to be performed in subsequent MS scans. Rather, only a few milliseconds of ions are introduced into the Orbitrap before the TWs are stopped. This means the Orbitrap can perform mass analysis with its shortest injection time (at a specified mass resolution setting) despite the initial SLIM separation time potentially being longer than the fastest Orbitrap injection time.

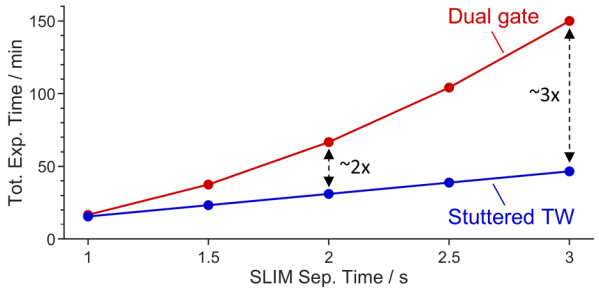


Figure 5: Comparison of the estimated total experiment times of the (red trace) stuttered TW scanning method and (blue trace) dual-gated scanning method as a function of SLIM separation time. $\Delta t_{dual\text{-}gate}$ = 1 ms.

A plot of estimated total experiment times vs SLIM separation times is given in **Figure 5** to better illustrate this point. The plot shows five total experiment times estimated from SLIM separation times of 1, 1.5, 2, 2.5, and 3 seconds. The total experiment times for the dual-gated experiments (**Figure 5**, red trace) were estimated by assuming a 1 ms step size, which is common, and an average of one scan per step. If the dual-gated SLIM separation time is 1 second, 1000 steps (in 1 ms increments) are required to sample the entire IMS spectrum. Since the Orbitrap injection time must also be equal to the IMS separation time, the total experiment time is ~16.7 minutes. However, if the dual-gated SLIM separation time is increased to 2 seconds,

2000 steps (in 1 ms increments) are required to sample the entire IMS spectrum. This also means that the Orbitrap injection time must also be set to 2 seconds, and therefore the total experiment time is 2*2000 = 4000 seconds, which is ~66.6 minutes. It is likely easy to imagine that these lengthy dual-gated SLIM-Orbitrap experiments can be prohibitive. Additionally, the dual-gated scanning technique also requires a continuous introduction of ions. Such long experiments will also consume high amounts of sample, and such large sample quantities are not available for samples such as single cells.

However, the total experiment times of the stuttered TW scan (**Figure 5, blue trace**) are lower than those of the dual-gated scanning technique. This occurs because the Orbitrap injection time is not required to be equal to the IMS separation time and can thus be set to the fastest possible time, which is 1 second for the Q-Exactive Orbitrap. Each time the stuttered TW scan is on, an injection time of 1 second can be used, regardless of SLIM separation time. If the SLIM separation time is 2 seconds, there are still ~2000 steps for the stuttered TW scanning method to sample across. However, the main difference between the stuttered TW and dual-gated scanning methods is that the number of steps is multiplied by 1 second, not 2 seconds. The Orbitrap injection time is unchanged even if the initial separation time before stopping the TWs is longer than 1 second. Depending on the experiment, the total ion mobilogram may contain ions arriving before the TWs are stopped, or it may not contain any ion signal if the TWs are stopped after 1 second. Note that these estimations do not include commonly implemented practices to reduce total experiment times, such as beginning dual-gated experiments at a $t \neq 0$ start time. However, the total experiment times of the dual-gated scanning technique will always be longer than the stutter TW scanning method if the IMS separation time is longer than the MS injection time.

## 3.4 Charge-transfer reactions when analyzing multiply charged peptides

The stuttered TW scanning method was also used to analyze a mixture of longer sequence peptides that typically exhibit singly and multiply charged ions in SLIM experiments. Overlaid EIMs of five peptides (1+ and 2+ charge states) are shown in **Figure 6**. Note that the stuttered TW conditions used in this experiment caused ions to “surf” out of the SLIM and not undergo additional separation after the stuttering process was started. Surprisingly, many peptides exhibited overlapping peaks corresponding to 1+ and 2+ charge states. Peaks corresponding to the 1+ charge states are expected to exhibit much longer arrival times than the 2+ charge states, and thus the data implies that ions with 2+ charge states are reducing to the 1+ charge state. To explore this further, experiments were performed using a shorter initial separation time (100 ms vs 200 ms). The result was that most ions were either not detected or small amounts of 1+ charge states were observed. The observation of charge transfer reactions for multiply charged peptides is an undesirable effect of the long times ions spend inside the SLIM.

Unfortunately, time did not allow for the problem of charge transfer reactions to be solved. However, solving this issue would presumably allow any experiments that require ions to spend long times inside the SLIM to be performed, including the analysis of ultralow volumes of sample. Future efforts will explore solutions to this issue, such as changing the SLIM board material to non-outgassing material and cooling the system to limit the energy available to cause a reaction.

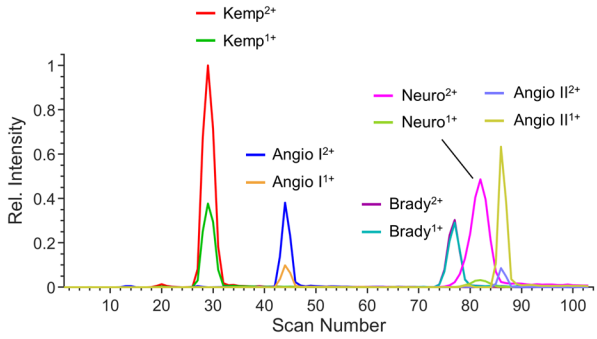


Figure 6: Overlaid EIMs of kemptide, angiotensin I, bradykinin, neurotensin, and angiotensin II acquired using the stuttered TW scanning method. $TW_{accum}$ = 104 m/s, 1 $V_{0\text{-}p}$, 100 ms. $TW_{sep}$ = 104 m/s, 15.5 $V_{0\text{-}p}$, 200 ms. $TW_{stutter}$ = 8 m/s, 5 $V_{0\text{-}p}$, 6 ms on-time.

## 3.5 The effects of TW phase on ion transmission efficiency during rerouting experiments

All experiments in this study were performing using SLIM boards possessing a new tee design that was designed to provide better ion transmission efficiencies during cyclic IMS separations than the conventional ion switch. The idea was that an independent TW with a reversible direction can be used to dictate whether ions are sent to the Orbitrap for high-resolution mass analysis (e.g., forward direction) or to the reroute path for additional IMS separation (e.g., reverse direction). The tee design does not use DC blocking barriers or non-intersecting TW tracks, both of which have been surmised to potentially cause peak broadening. However, the SLIM was designed such that ions entered the tee region via a 90° turn. It was therefore important to consider the phasing of the TWs when changing TW direction. An illustration of the TW phasing in and around the new tee region under three different TW conditions is shown in **Figure 7**. The numbers 1 through 8 represent the sequence that waveforms follow to create the TWs. Each number represents a 45° phase shift. The phasing of the TWs at the 90° turns in most reported SLIM designs follows a pattern where the last TW electrodes in one track are 45° phase-shifted from the first TW electrodes located at the edge of the intersecting track. These two sets of TW electrodes are highlighted in **Figure 7A** with red circles. If the final TW electrode possess a number 8 (e.g., Φ= 315°), then the first TW electrode of the 90° turn will possess a number 1 (e.g., 0°). The SLIM boards were designed to send ions to the Orbitrap by default, and this default TW phasing is represented in **Figure 7A**. However, it was hypothesized that the TW in the tee region should also be phase-shifted when its direction is reversed so that the same TW phasing as used in the fifty other 90° turns could also be applied to the tee. Reversing the TW direction at the 90° turn without also phase-shifting it would result in a phase mismatch, which is illustrated in **Figure 7B**. To achieve a conventional TW phasing at the 90° turn while the TW direction is reversed, the TWs in the tee region should be phase-shifted by 180° (**Figure 7C**). Using TWs with phase mismatches at the 90° turns have long been suspected to cause peak broadening and potentially ion losses, but there are currently no reported studies (ion trajectory simulations or experiments) that explored the effects of TW phase at the 90° turns. The new SLIM boards in this study provided a good way to study how TW phasing at the turns affects IMS separation quality, and thus a systematic study of TW phase at the turns was performed. It is noted that the study is not perfect because it was not straightforward to conceive of a way to phase-shift all the turns in the SLIM. In lieu of this, only the TW in the tee region was phase-shifted. However, even

this nonideal way of exploring TW phase shifts at the 90° turns caused observable effects inside the SLIM.

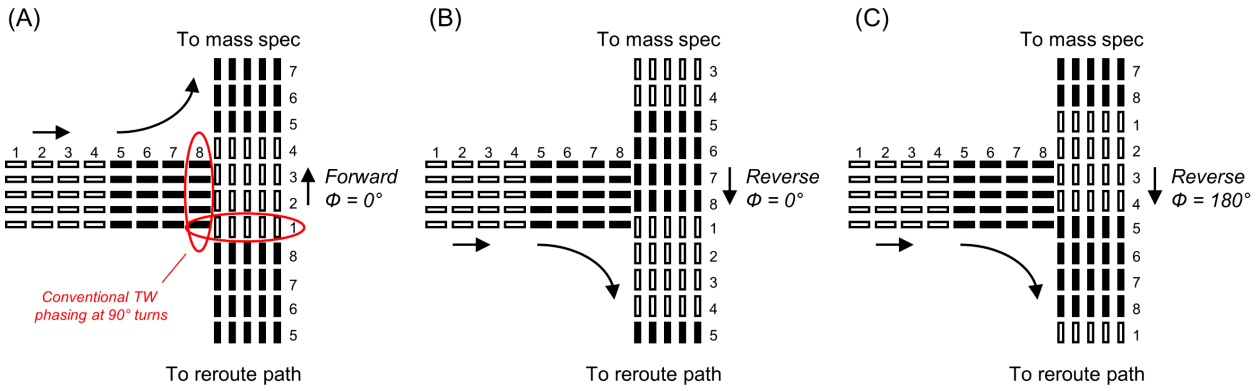


Figure 7: Illustrations of the TW phasing at the switching tee region. (A) Forward direction towards the MS. The red circles highlight the phasing of the final TW electrodes in one track and the first TW electrodes in the intersecting track. (B) Reverse direction towards the SLIM reroute path. (C) Reverse direction with 180° phase shift towards the SLIM reroute path. The black and white rectangles represent TW amplitudes of $+V_{0\text{-}p}$. and $-V_{0\text{-}p}$, respectively.

The effect of TW phasing at the 90° turn in the tee region of the SLIM was evaluated by performing IMS separations of the reverse peptides using five passes through the SLIM (i.e., 55-meter cyclic separations). The ions traversed two phase-shifted 90° turns each time they were rerouted for another pass through the SLIM, meaning that ions encountered eight total phase-shifted 90° turns per IMS experiment out of a total of 250 turns. On the fifth pass through the SLIM, ions were to the Orbitrap using TW phasing conventionally used at 90° turns (see **Figure 7A**). IMS separations were performed using the new stuttered TW scanning method, and overlaid EIMs of *m/z* 491 acquired using eight different phase-shifts (0°, 45°, 90°, 135°, 180°, 225°, 270°, 315°) are shown in **Figure 8A**. Illustrations of the corresponding TW phasing for each EIM is shown in **Figure 9**. Since 55-meters of SLIM path length was used for these experiments, the separation between both peaks was noticeably higher compared to the previous 11-meter separations. The average resolution of the reverse peptides across all eight conditions was 5.30, which was ~2.4x higher than calculated for the 11-meter pass previously calculated and falls in line with the expectation that resolution scales with the square root of IMS path length ($\sqrt{(55 \div 11)} = 2.24$).(Giles et al. 2019, 8572) While many of the EIMs largely overlapped, a few outliers stood out. The clearest outlier corresponded to a TW phase shift of 315° (**Figure 8A**, light green trace), which exhibited the broadest peaks (**Figure 8B**) and the longest arrival times (**Figure 8C**) out of the eight TW phases evaluated. This observation supports the hypothesis that TW phasing mismatches at the 90° turns can cause ions to experience a greater number of rollover events, which in turn leads to peak broadening. In contrast, IMS peaks acquired using a TW phase shift of 135° (**Figure 8**, orange trace) exhibited the narrowest peaks and shortest arrival times. Ions exhibiting faster arrival times typically exhibit the narrowest peaks, so it is most desirable to use TW conditions that move ions through the SLIM most quickly. This experiment indicates that 135° is the most desirable TW phase to use when reversing the TW at the tee region.

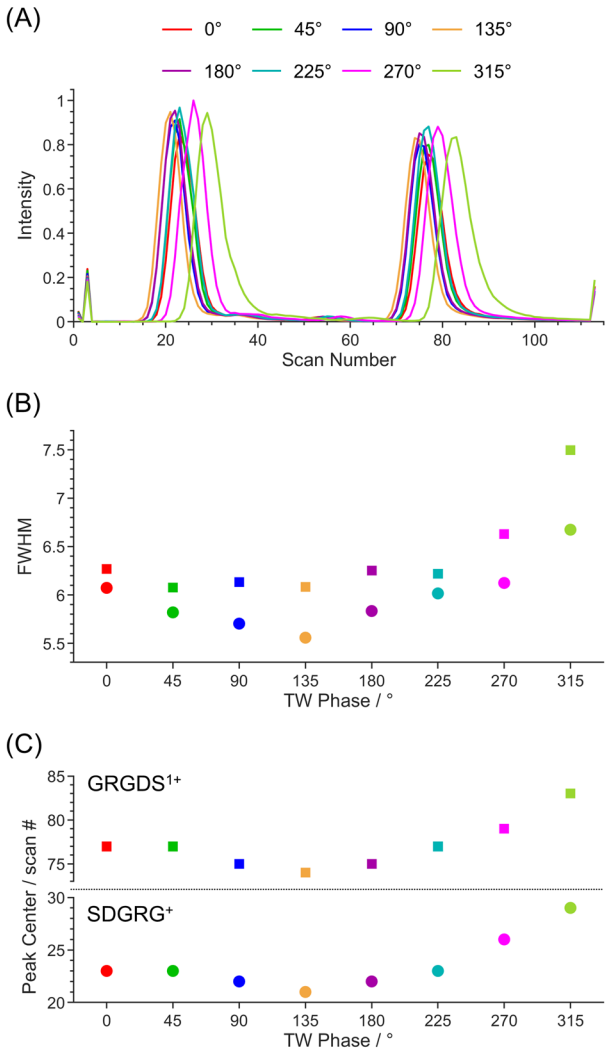


Figure 8: (A) Overlaid EIMs of *m/z* 491 showing the effect of using eight different TW phases in the new tee region. Corresponding plots of (B) FWHM and (C) peak centers as a function of TW phase. SLIM length = 55-meters.

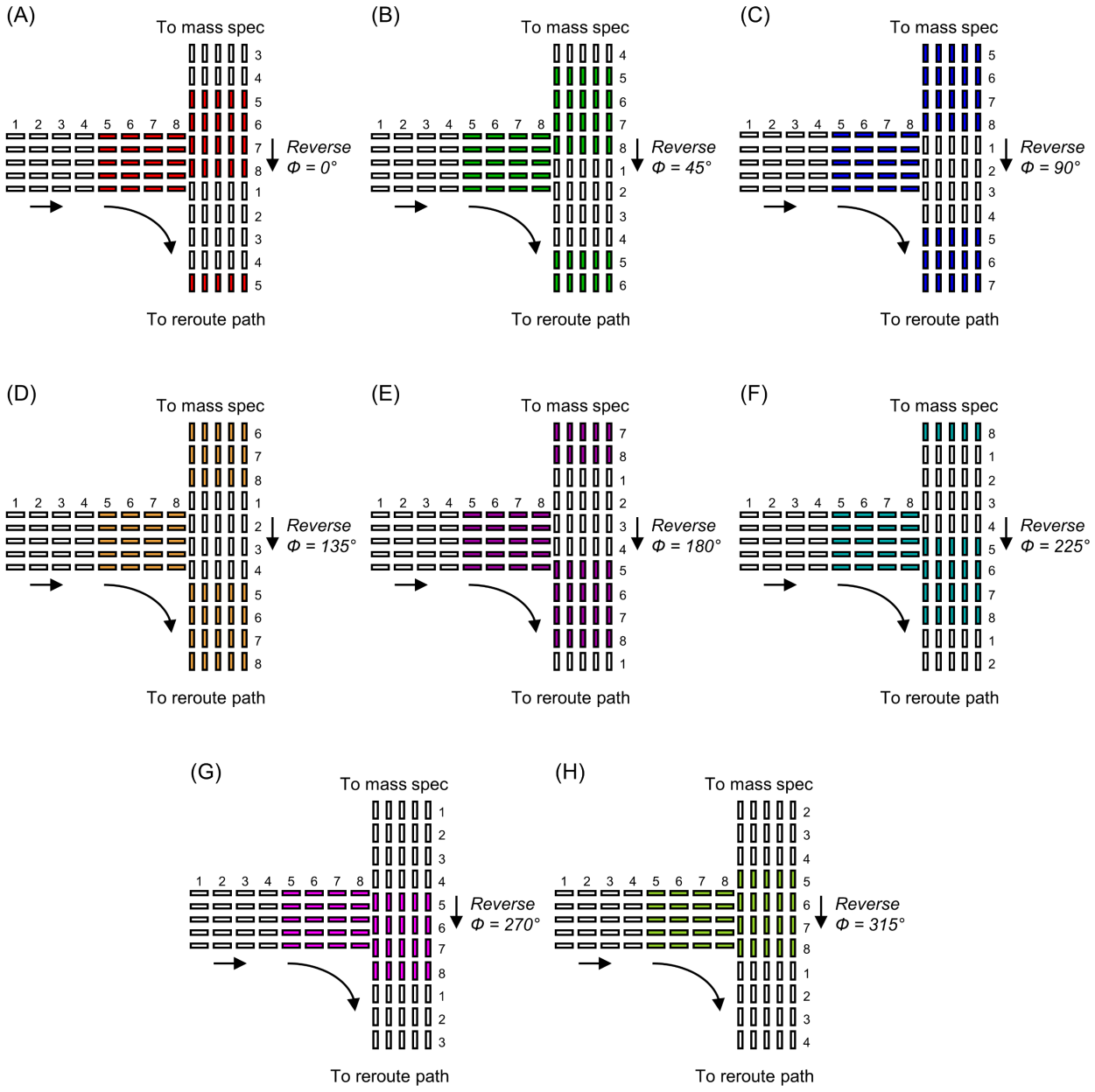


Figure 9: Illustrations of eight different TW phasings applied to the new tee region of the SLIM.

Since the experiments utilized a small number of 90° turns, it is not entirely unexpected that the observable effects of the phase-shifting the TWs at the 90 turns was also small. However, the effects were also noticeable, and further studies using larger numbers of 90° turns would provide more insights. The ideal way to study the effects of TW phasing at 90° turns would be to phase-shift all the TWs in the SLIM via a simple command or wire swap. This would allow the same SLIM boards and parameters to be used in each experiment. However, the authors of this study could not think of a straightforward way to implement this approach. An alternate way to experimentally validate which TW phasing at the 90° turns is optimal would be to manufacture eight different SLIM boards with all the 90° turns in the SLIM designed with the different phase shifts. This would allow hundreds of 90° turns to be evaluated, but unfortunately this kind of study could produce results that are difficult to compare due to repeated instrument alterations, vacuum venting cycles, manufacturing variability of the SLIM boards, etc.

# 4.0 Conclusions

A new high ion utilization efficiency method was developed for TWIMS systems for analyzing ultralow volume samples with high-resolution IMS and high-resolution MS. The new method showed similar resolutions, peak shapes, and peak intensities compared to a dual-gated scanning method for standard, stable ions. The new method was also demonstrated to be faster than the dual-gated scanning method in cases where the IMS separation time is longer than the MS analysis time, which can occur during cyclic IMS operation. A new SLIM design and operation facilitated high ion utilization efficiency during cyclic operation, and the design will likely be used in future SLIM designs.

The new stuttered TW scanning method exhibited charge reduction reactions for a mixture of standard peptides, and future efforts will explore what components in the system contribute to the charge reduction process and how the reactions can be avoided. Successfully eliminating side reactions during the stuttered TW scanning method will allow for ultralow volume samples, such as single cells, to be analyzed with high-resolution IMS / high-resolution MS platforms. The data from such platforms will provide a wealth of information about cellular constituents that cannot currently be obtained.

# 5.0 References

Blaženović, Ivana, Tong Shen, Sajjan S. Mehta, Tobias Kind, Jian Ji, Marco Piparo, Francesco Cacciola, Luigi Mondello, and Oliver Fiehn. 2018. “Increasing Compound Identification Rates in Untargeted Lipidomics Research with Liquid Chromatography Drift Time-Ion Mobility Mass Spectrometry.” *Analytical Chemistry* 90 no. 18 (August): 10758-64. https://doi.org/10.1021/acs.analchem.8b01527.

Garimella, Sandilya V. B.; Yehia M. Ibrahim, Ian K. Webb, Andreas B. Ipsen, Tsung-Chi Chen, Aleksey V. Tolmachev, Erin S. Baker, Gordon A. Anderson, and Richard D. Smith. 2015. “Ion manipulations in structures for lossless ion manipulations (SLIM): computational evaluation of a 90° turn and a switch.” *Analyst* 140 no. 20 (August): 6845-52. https://doi.org/10.1039/C5AN00844A.

Giles, Kevin, Jakub Ujma, Jason Wildgoose, Steven Pringle, Keith Richardson, David Langridge, and Martin Green. 2019. “A Cyclic Ion Mobility-Mass Spectrometry System.” *Analytical Chemistry* 91 no. 13 (July): 8564-8573. https://doi.org/10.1021/acs.analchem.9b01838.

Hollerbach, Adam L., Patrick W. Fedick, and R. Graham Cooks. 2018. “Ion Mobility–Mass Spectrometry Using a Dual-Gated 3D Printed Ion Mobility Spectrometer.” *Analytical Chemistry* 90 no. 22 (October): 13265-72. https://doi.org/10.1021/acs.analchem.8b02209.

Hollerbach, Adam L., Yehia M. Ibrahim, Vanessa Meras, Randolph V. Norheim, Adam P. Huntley, Gordon A. Anderson, Thomas O. Metz, Robert G. Ewing, and Richard D. Smith. 2023. “A Dual-Gated Structures for Lossless Ion Manipulations-Ion Mobility Orbitrap Mass Spectrometry Platform for Combined Ultra-High-Resolution Molecular Analysis.” *Analytical Chemistry* 95 no. 25 (June): 9531-8. https://doi.org/10.1021/acs.analchem.3c00881.

Karasek, Francis W., Herbert H. Hill, and Sanghyeon H. Kim. 1976. “Plasma chromatography of heroin and cocaine with mass-identified mobility spectra.” *J. Chromatogr. A* 117 (February): 327-36. https://doi.org/10.1016/0021-9673(76)80009-X.

Luo, M., Yadong Yin, Zhiwei Zhou, Haosong Zhang, Xi Chen, Hongmiao Wang, and Zheng-Jian Zhu. 2023. “A mass spectrum-oriented computational method for ion mobility-resolved untargeted metabolomics.” *Nature Communications* 14 no. 1813 (March). https://doi.org/10.1038/s41467-023-37539-0.

Pu, Yi, Mark E. Ridgeway, Rebecca S. Glaskin, Melvin A. Park, Catherine E. Costello, and Cheng Lin. 2016. “Separation and Identification of Isomeric Glycans by Selected Accumulation-Trapped Ion Mobility Spectrometry-Electron Activated Dissociation Tandem Mass Spectrometry.” *Analytical Chemistry* 88 no. 7 (March): 3440-3. https://doi.org/10.1021/acs.analchem.6b00041.

Wojcik, Roza, Gabe Nagy, Isaac K. Attah, Ian K. Webb, Sandilya V. B. Garimella, Karl K. Weitz, Adam Hollerbach, et al. 2019. “SLIM Ultrahigh Resolution Ion Mobility Spectrometry Separations of Isotopologues and Isotopomers Reveal Mobility Shifts due to Mass Distribution Changes.” *Analytical Chemistry* 91 no. 18 (September):11952-11962. https://doi.org/10.1021/acs.analchem.9b02808.

Zhou, Li, Bingfang Yue, David V. Dearden, Edgar D. Lee, Alan L. Rockwood, and Milton L. Lee. 2003. “Incorporation of a Venturi Device in Electrospray Ionization.” *Analytical Chemistry* 75 no. 21 (November): 5978-83. https://doi.org/10.1021/ac020786e.

# Pacific Northwest National Laboratory

902 Battelle Boulevard
P.O. Box 999
Richland, WA 99354

1-888-375-PNNL (7665)

***www.pnnl.gov***